Mineral. Deposita 31, 374–385 (1996)

MINERALIUM DEPOSITA

The age and thermal history of Cerro Rico de Potosi, Bolivia

C.G. Cunningham[1], R.E. Zartman[2], E.H. McKee[3], R.O. Rye[4], C.W. Naeser[5], O. Sanjinés V.[6], G.E. Ericksen[7], F. Tavera V.[8]

[1] U.S. Geological Survey, 954 National Center, Reston, Virginia 22092
[2] U.S. Geological Survey, Box 25046, Mail Stop 963, Denver Federal Center, Denver, Colorado 80225
[3] U.S. Geological Survey, 345 Middlefield Road, Menlo Park, California 94025
[4] U.S. Geological Survey, Box 25046, Mail Stop 963, Denver Federal Center, Denver, Colorado 80225
[5] U.S. Geological Survey, 926A National Center, Reston, Virginia 22092
[6] Servicio Geológico de Bolivia (GEOBOL), Calle Federico Zuazo 1673, Casilla 2729, La Paz, Bolivia
[7] U.S. Geological Survey, 954 National Center, Reston, Virginia 22092 (deceased 14 January 1996)
[8] Servicio Geológico de Bolivia (GEOBOL), Calle Federico Zuazo 1673, Casilla 2729, La Paz, Bolivia

Received: 14 October 1995 / Accepted: 29 January 1996

Abstract. Cerro Rico de Potosi, Bolivia, is the world's largest silver deposit and has been mined since the sixteenth century for silver, and for tin and zinc during the twentieth century, together with by-product copper and lead. The deposit consists primarily of veins that cut an altered igneous body that we interpret to be a dacitic volcanic dome and its underlying tuff ring and explosion breccia. The deposit is compositionally and thermally zoned, having a core of cassiterite, wolframite, bismuthinite, and arsenopyrite surrounded by a peripheral, lower-temperature mineral assemblage consisting principally of sphalerite, galena, lead sulfosalt, and silver minerals. The low-temperature assemblage also was superimposed on the high-temperature assemblage in response to cooling of the main hydrothermal system. Both the dacite dome and the ore fluids were derived from a larger magmatic/hydrothermal source at depth. The dome was repeatedly fractured by recurrent movement on the fault system that guided its initial emplacement. The dome was extruded at 13.8 ± 0.2 Ma (2σ), based on U-Th-Pb dating of zircon. Mineralization and alteration occurred within about 0.3 my of dome emplacement, as indicated by a $^{40}Ar/^{39}Ar$ date of 13.76 ± 0.10 Ma (1σ) for sericite from the pervasive quartz-sericite-pyrite alteration associated with the main-stage, high-temperature, mineralization. The last thermal event able to reset zircon fission tracks occurred no later than 12.5 ± 1.1 Ma (1σ), as indicated by fission-tract dating. Minor sericite, and magmatic-steam alunite veins, were episodically formed around 11 Ma and between 8.3 and 5.7 Ma; the younger episodes occurring at the time of extensional fracturing at Cerro Rico and widespread volcanism in the adjacent Los Frailes volcanic field. None of these younger events appear to be significant thermal/mineralizing events; the exceptionally flat thermal release pattern of ^{39}Ar from sericite and the results of the fission-tract dating of zircon show that none of the younger events was hot enough, and lasted long enough, to cause significant loss of Ar or annealing of zircon fission tracks. U-Th-Pb dating of zircon cores indicates a Precambrian progenitor for some zircons, and REE analyses of dated samples of hydrothermally altered dacite show the presence of a prominent positive Eu anomaly, which constrains interpretations of the origin and evolution of the magmatic/hydrothermal system.

Cerro Rico de Potosi, Bolivia, has produced an estimated 30 000 to 60 000 tonnes of silver from high-grade Ag and Ag-Sn veins, and it is estimated that at least that much silver still remains (Miller and Singewald 1919; Bernstein 1987, 1989; Suttill 1988). The oxidized silver ores mined in the sixteenth century had grades of as much as 30–40% Ag (Omiste 1893). Silver mining reached a peak during the sixteenth and seventeenth centuries, and Potosi reportedly became the second most populous city in the western world and was the site of the first mint in the Americas. The Spaniards were only interested in precious metals and any tin, copper, lead, and zinc produced was used for amalgams to make utensils and church bells (Berry 1939). Low silver prices about 1891 resulted in a change from mining silver to mining tin (Evans 1940), and Potosi was mined almost exclusively for tin from then until the tin market collapsed in 1985. Gold is not known to be present in the deposit in recoverable quantities.

Currently, Cerro Rico de Potosi is a hill honeycombed with underground workings, some of which now host small-scale mining operations, and many mine dumps, two of which are being leached for Ag. Recent evaluations indicate that Cerro Rico is pervasively mineralized and contains about 442 million tonnes of disseminated ore having an average grade of 106 g/tonne Ag and 0.1–0.18% Sn; an additional 100 million tonnes of material of similar grade is present in alluvium/colluvium and mine dumps (Bernstein 1989).

Cerro Rico is situated within the Bolivian tin belt, which extends throughout Bolivia from southernmost Peru to northernmost Argentina. The many Sn deposits in

Correspondence to: C.G. Cunningham

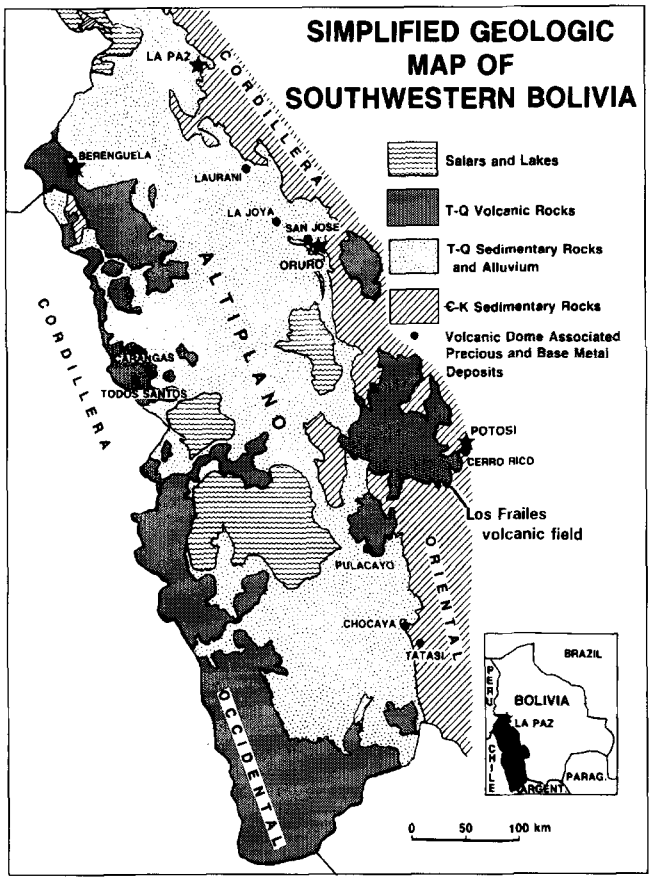

Fig. 1. Simplified geologic map of southwestern Bolivia

this belt are associated with peraluminous igneous rocks, mostly large granitic plutons in the northern part and subvolcanic intrusions and volcanic domes in the central and southern part (Ahlfeld 1967; Turneaure 1971; Urquidi-Barrau 1989; Ericksen et al. 1990). Potosi is in the central part of the tin belt, about 420 km southeast of La Paz. It is in the Cordillera Oriental, east of the Altiplano (Fig. 1), and just east of the Los Frailes volcanic field. Seen from the city of Potosi, which it adjoins to the south, Cerro Rico appears as a conical hill consisting of a reddish-brown (iron-oxide stained) silicified cap above slopes of grayish-blue altered dacite covered with many mine dumps.

Cerro Rico has been variously interpreted to be a stock, subvolcanic intrusion, or a dome (Lindgren and Creveling 1928; Turneaure 1960a; Sillitoe et al. 1975; Francis et al. 1981). Isotopic dates for veins and altered wallrock range from 18.7 to 7.5 Ma, with alteration-related dates 14 to 12 Ma (Grant et al. 1979; Schneider and Halls 1985; Schneider 1987). The basement rocks are Ordovician clastic sediments. The mushroom-shaped Cerro Rico igneous body both cross-cuts and overlaps a percursor sequence of heterolithic breccia and overlying dacitic tuff (Fig. 2). Because of the intense hydrothermal alteration, the Cerro Rico dacite has previously not been directly dated. In this study, we interpret the dacite to be a volcanic dome, that the underlying breccia and tuff resulted from explosive eruptions that preceded dome emplacement, and that the dome was extruded at 13.8 ± 0.2 Ma and mineralized shortly thereafter. The dome is considered too young to be a ring dome of the nearby Kari Kari caldera dated at 20.8 Ma, although it may have been intruded along part of the caldera fracture system.

Previous major studies of Cerro Rico de Potosi include Lindgren and Creveling (1928), Turneaure 1960a,b), Ahlfeld and Schneider-Scherbina (1964), Sillitoe et al. (1975), Grant et al. (1979), Francis et al. (1981), Sugaki et al. (1983), Schneider (1985), and Bernstein (1987, 1989).

Geologic setting

An east-west cross section through Cerro Rico de Potosi, near its peak and based on centuries of mining and drilling data, shows the major geologic relations (Fig. 2). The oldest rocks in the area are black to gray, generally steeply dipping, Ordovician phyllites with minor sandstone interbeds. A few kilometers east of Cerro Rico is the resurgent dome of the 20.8 Ma Kari Kari caldera, which consists mostly of garnet-bearing welded tuffs (Francis et al. 1981; Schneider 1985). In the vicinity of Cerro Rico is a sequence of tuffs, breccias, and conglomerates that appear to be unique to the area and have been collectively called the Cerro Rico Formation (Turneaure 1960a). The lithologic units that make up this sequence (Fig. 2) include the Pailaviri conglomerate, Venus breccia, and Caracoles tuff (Evans 1940; Turneaure and Marvin 1947; Turneaure 1960a). The basal Pailaviri conglomerate is combined with the overlying Venus breccia in Fig. 2. The conglomerate contains rounded pebbles of many lithologies including shale, quartzite, and igneous rock, and correlates with similar strata as much as 10 km away (Turneaure 1960a). The Venus breccia, which is up to 100 m thick, contains angular fragments of Ordovician phyllite and sparse dacite in a matrix of tuff and small fragments of phyllite. The overlying Caracoles tuff consists of locally reworked, well-bedded ash with interlayered breccias. It is up to 300 m thick and is cut by the central feeder dike of the Cerro Rico dome; as shown in Fig. 2, the dome flares outward over this tuff (Turneaure and Marvin 1947; Turneaure 1960a). The Caracoles tuff contains sandy layers in which are plant fossils that have been variously classified as being middle Tertiary to Pliocene in age (Steinmann 1922; Brüggen 1934; Berry 1939).

The Cerro Rico dacite dome is a mushroom-shaped body measuring 1700 m by 1200 m at the surface, narrowing to a 100-m-wide dike, striking about N 12 W, at depth (Turneaure 1960a). The dacite originally consisted of 3–5 mm phenocrysts of quartz, plagioclase, K-feldspar, and biotite in a fine-grained matrix of the same minerals. It has been pervasively altered to a rock consisting of sericite, kaolinite, chlorite, and primary and secondary quartz, and disseminated pyrite, the typical assemblage of quartz-sericite-pyrite (QSP) alteration. The silicified cap that makes up the uppermost part of the conical hill consists essentially of residual and secondary quartz. The siliceous cap contains prominent cavities after leached feldspars and oxidized pyrite cubes and is thus similar in appearance to the "vuggy silica" of acid sulfate deposits such as Summitville, Colorado (Stoffregen 1987; Rye et al. 1992). However, it has important differences in that, rather than the vertical aspect vuggy silica zones with their bordering, generally symmetrical, replacement alunite-kaolinite zones of acid-sulfate systems, the cap subhorizontally overlies, and is believed to be part of, the QSP-dominated ore body that formed by adularia-sericite type alteration. The subhorizontal base of the cap is generally parallel to what is interpreted to be the top of the dome and the cap has been leached by supergene solutions resulting from oxidation of its contained pyrite.

Cerro Rico ore deposit

Most of the Cerro Rico ore has been mined from veins that vary in width from a few tens of centimeters to several meters, although

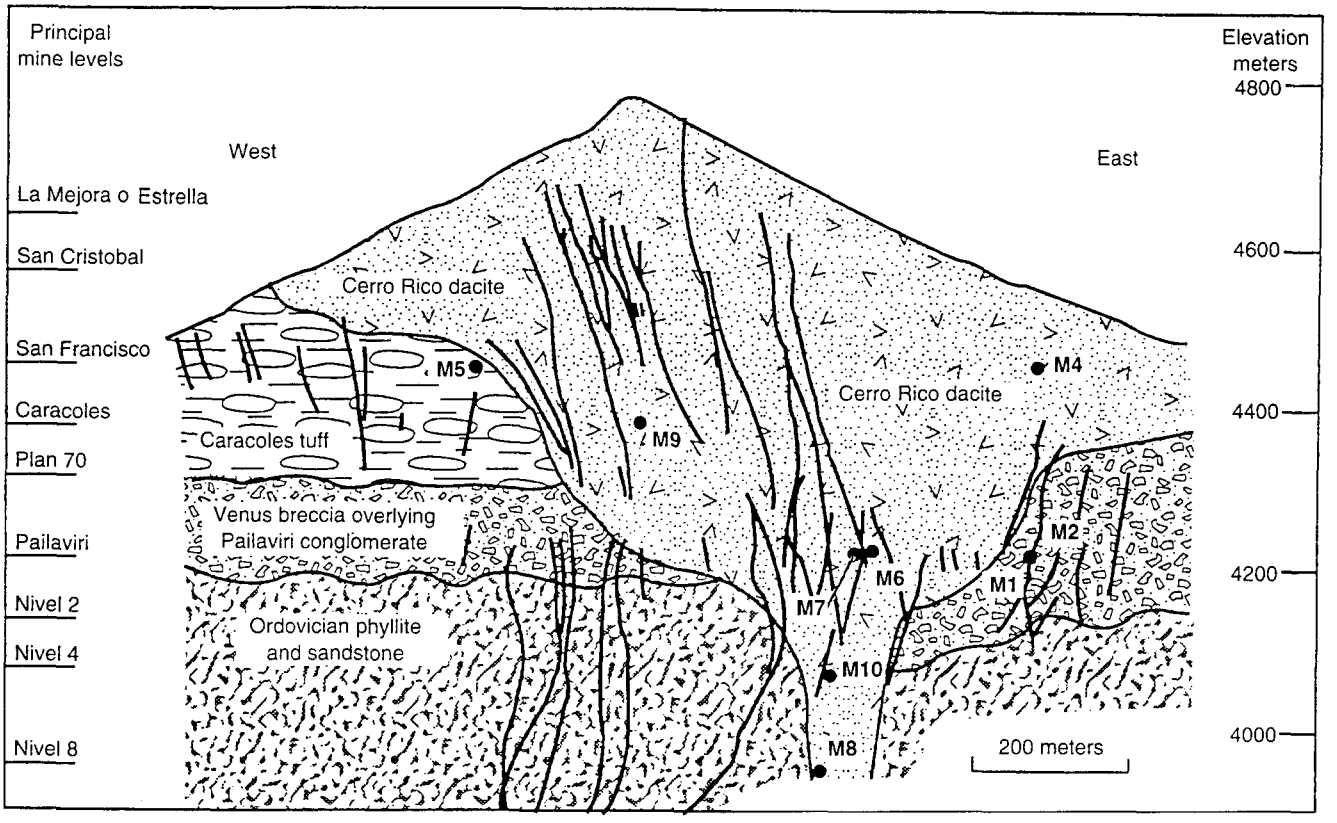

Fig. 2. East-west cross section through Cerro Rico de Potosi, Bolivia, showing principal veins and mine levels: locations of dated samples are projected onto the plane of the section. Sample M3 is from mine level 16. Based on mine maps from Compañia Mineria del Sur (COMSUR)

workable veins have an average width of about a meter (Lindgren and Creveling 1928). Shear zones consisting of swarms of veinlets also have been mined. Sillitoe et al. (1975) described pervasive microveinlets in the wallrock that they considered to represent porphyry style mineralization. The veins cut the underlying Ordovician phyllites, as well as the conglomerates, breccias, and tuff of the Cerro Rico Formation, and the Cerro Rico dacite dome (Fig. 2). Most of the veins strike northeast and dip steeply. The upper part of the dome contains a N 31° E-trending, 170-m-wide sheeted zone of closely spaced, narrow veins; other groups of veins trend N 53° E and N 6° E. Turneaure (1960a) presents a detailed description and structural analysis of the Cerro Rico veins.

The veins have been mined over a vertical distance of about 1150 m, from the summit (4824 m) to the − 16 level (3674 m), which is now flooded. The contact between the oxidized ore zone and the underlying primary sulfide ore zone is irregular and is located about 300 m below the summit of Cerro Rico. The oxidized ores above the Caracoles level (Fig. 3) had been largely mined out by the early part of the twentieth century (Lindgren and Creveling 1928), with ore only remaining in pillars, fill, and sections of the veins isolated by cave-ins.

The Cerro Rico ores are spatially and temporally zoned (Turneaure 1960b). In the center, or core, of the deposit, high temperature minerals including cassiterite, wolframite, bismuthinite, and arsenopyrite were co-deposited. Surrounding the core, in the peripheral parts of the deposit, a lower temperature assemblage including sphalerite, galena, Pb-sulfosalts, and Ag-minerals are predominant. The principal Ag minerals near the top of the vein system are argentite, ruby silver, native silver, and supergene chlorargyrite, whereas at depth, tetrahedrite is the most abundant Ag-bearing mineral (Miller and Singewald 1919; Lindgren and Creveling 1928). Repeated fracturing and multiple hydrothermal events are recorded

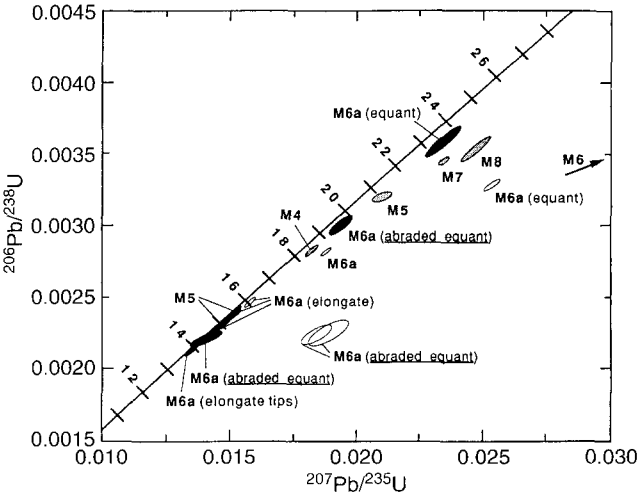

Fig. 3. $^{206}Pb/^{238}U$–$^{207}Pb/^{235}U$ concordia diagram for zircon from Cerro Rico de Potosi, Bolivia, that indicates an age of 13.8 ± 0.2 Ma for the emplacement of the volcanic dome. Color of zircon fractions indicated by ellipse pattern (*white* = colorless; *black* = yellow; *stippled* = mixed)

by successive cross-cutting veins. Base-metal sulfides, Ag-bearing minerals, and Pb-sulfosalts, are in paragenetically late associations with earlier minerals or occur in veins cutting earlier high-temperature veins in the core. Stannite and chalcopyrite are present between the high- and low-temperature assemblages (G. Steele, written

Table 1. Descriptions and mine locations of analyzed samples from Cerro Rico de Potosi

M 1	Vein of hard, cream-colored, fine-grained alunite containing disseminated, euhedral pyrite crystals. Veins of sulfide minerals, including pyrite, arsenopyrite, cadmium-rich tennantite, greenockite, sphalerite, ferroan tetrahedrite, and stannite, cut the alunite and are cut by alunite veinlets. Pailaviri level O, main drift south
M 2	Vein of hard, cream-colored, fine-grained alunite about 0.5 m wide; contains spheres of clear, radiating alunite crystals. No sulfides present. Pailaviri level O, main drift south, about 2 m north of M 1
M 3	Vein of hard, cream-colored, fine-grained alunite and woodhouseite containing disseminated sulfides, including pyrite and sphalerite. Vein has a selvage of pyrite-quartz-cassiterite. Mine level 16
M 4	Altered dacite porphyry containing kaolinite and sericite. Brac 4500 level, 4, 641N., 5, 540E
M 5	Altered dacite porphyry with red, oxidized groundmass and feldspars converted to kaolinite. San Francisco level, 4, 790N., 4, 800E
M 6	Altered dacite containing disseminated sericite and pyrite. M 6a is a recollected 100 kg sample. Pailaviri level 0, 5, 000N., 5, 285E
M 7	Altered dacite containing disseminated pyrite. Pailaviri level 0, 5, 323N., 5, 241E
M 8	Altered dacite containing disseminated pyrite. Mine level 8, 5, 200N., 5, 195E
M 9	Altered dacite with feldspars converted to sericite. Caracoles level, 5, 010N., 5, 013E
M 10	Altered dacite with feldspars converted to sericite. Mine level 4, 5, 228N., 5, 248E

communication 1995), and are locally associated with cassiterite (Turneaure 1960b). The zoning, including telescoping of the ore, is similar to that at the Julcani, Peru deposit (Rye 1993; Deen et al. 1994).

Fluid inclusion data is scanty. Sugaki et al. (1983, 1988) reported that fluid inclusions in quartz, associated with cassiterite, from the Bolivar "2" vein on the Pailaviri level, have homogenization temperatures of 286–315 °C and salinities of 13.5–13.0 wt.% NaCl equivalent. These authors reported homogenization temperatures in quartz with pyrite and chalcopyrite, from the Don Mauricio vein on the same level, of 243–282 °C and 4.7–11.7 wt.% NaCl equivalent. They also reported homogenization temperatures in quartz from the Utne-2 vein as 231–371 °C, with salinities of 4.4–19.7 wt% NaCl equivalent, and from the Utne-4 vein as 271–329 °C, with 9.2–9.5 wt. percent equivalent NaCl; the mineral associations and sample locations of this latter data are not specified.

Tourmaline is reported to occur in the altered wall rock and rarely in the veins (Turneaure 1960a). It is associated with cassiterite and formed during the earliest stage of mineralization (Sugaki et al. 1983). Tourmaline apparently is most abundant deep in the deposit, as is boron (>2000 ppm in sample M 8).

Several generations of alunite veins are present, and those exposed in the mine are generally described as being paragenetically late. Lindgren and Creveling (1928) reported some alunite as being hypogene based on its association with cassiterite. Samples of alunite veins collected for geochronology, geochemistry, and stable isotope determinations are described in Table 1 and their locations shown on Fig. 2. The analyzed vein alunite is confirmed as being hypogene, and both hand-sample examination and microprobe analyses show it contains, and is cut by, minor quantities of pyrite, arsenopyrite, cadmium-rich tennantite, greenockite, sphalerite, ferroan tetrahedrite, and stannite (Robert Seal, written communication 1991). Additional evidence of the hypogene nature of the alunite veins is given by stable isotope data for both alunite and associated pyrite (Table 2). These data are typical of *magmatic steam* alunites (Rye et al. 1992), which originate from bursts of steam of evolved magmatic fluids. The isotopic compositions indicating a magmatic steam origin are δD values of -69 and -74‰. indicating a magmatic source for the fluids and $\delta^{34}S$ values typical of the bulk sulfur in the system ($\delta^{34}S$ values for the alunite are 3.7 to 5.1‰. whereas those for pyrite are 1.9 to 2.8‰.) indicating a lack of equilibrium between sulfur species and a SO_2 dominant vapor phase in the system *during alunite deposition.* Unrelated, late, secondary alunite veinlets are present in the oxidized ores (Schneider 1985).

Table 2. Stable isotope analyses of alunite and pyrite in samples M 1 and M 3, Cerro Rico de Potosi, Bolivia

	M 1	M 3
$\delta^{18}O_{SO_4}$	8.0	12.4
$\delta^{18}O_{OH}$	4.5	8.4
$\Delta^{18}O_{SO_4-OH}$[a]	3.5 = 290 °C	4.0 = 240 °C
δ D	−69	−74
$\delta^{34}S_{SO_4}$	5.1	3.7
$\delta^{34}S_{PY(disseminated)}$	1.9	2.8

[a] Temperature from Stoffregen et al. 1994

Geochronology

The age of volcanic activity and the timing and extent of the multiple episodes of mineralization of Cerro Rico are important factors in understanding the magmatic/hydrothermal history of the deposit, an understanding that should be of aid to mineral exploration in this part of the Andes. The Cerro Rico dacite is pervasively altered, and it has been additionally affected by supergene oxidation down to about the Caracoles level (Fig. 2); consequently, previous K-Ar studies of the dacite and alunite dated aspects of alteration, mineralization, and perhaps supergene oxidation rather than the initial, dome-forming, igneous activity. Previous reported ages range from 18.7–7.5 Ma. They include four sericitized whole rock K-Ar determinations by Grant et al. (1979) of 13.6 ± 0.4 Ma and 14.1 ± 0.3 Ma (the two are each averages of duplicate argon analyses). These authors considered it unlikely that the dacite was emplaced much more than 1 my prior to sericitic alteration. Schneider (1985) reported K-Ar ages for 10 samples of alunite veins, ranging from 13.52–10.35 Ma; considering Ar and K analytical results, he interpreted the one having the lowest error as 12.59 ± 0.57 Ma. He also reported K-Ar dates of about 18.7 – 18.5 Ma from 2 samples of alunite veins from the

Table 3. Major element and selected trace element analyses of altered dacite from Cerro Rico de Potosi. Major element data in wt.%. Trace element data in (ppm)

Field number	M 4	M 5	M 6	M 7	M 8	M 9	M 10
Lab. number	W-255616	W-255617	W-255618	W-255619	W-255620	W-256090	W-256091
SiO_2	70.6	76.4	62.4	67.8	69.8	69.3	66.5
Al_2O_3	17.9	6.96	13.1	14.1	15.0	15.4	13.5
$FeTO_3$	0.51	9.61	10.8	6.42	5.91	2.45	7.69
MgO	0.25	< 0.10	0.36	0.39	0.40	0.20	0.23
CaO	0.04	0.08	0.03	0.04	0.05	0.10	0.04
Na_2O	< 0.15	< 0.15	< 0.15	< 0.15	0.22	< 0.15	< 0.15
K_2O	3.75	0.12	3.54	3.82	0.50	3.52	3.32
TiO_2	0.65	0.64	0.43	0.53	0.54	0.55	0.53
P_2O_5	0.49	0.51	0.25	0.44	0.40	0.44	0.33
MnO	0.02	< 0.01	0.01	0.02	< 0.01	0.02	0.04
LOI 925 °C	4.42	4.06	8.36	5.67	3.93	6.64	7.52
Sc	4.38	2.33	3.16	3.65	3.49	3.86	4.19
Cr	5.7	8.6	6.5	5.7	11.4	7.7	23.1
Co	3.64	0.53	5.35	1.79	1.88	3.61	6.21
Zn	559.0	25.9	893.0	171.0	348.0	1690.0	207.0
As	2.61	490.0	368.0	386.0	274.0	109.0	384.0
Rb	379.0	12.9	293.0	311.0	37.1	295.0	323.0
Sr	790.0	3430.0	559.0	363.0	49.0	100.0	84.0
Zr	160.0	210.0	104.0	149.0	175.0	161.0	146.0
Mo	< 4.0	< 4.0	< 6.0	< 4.0	< 4.0	< 6.0	4.5
Ag	< 0.5	50.0	3.0	1.0	< 0.5	< 0.5	< 0.5
Be	7.0	3.0	3.0	5.0	3.0	3.0	2.0
Bi	< 10.0	< 10.0	20.0	10.0	< 10.0	< 10.0	< 10.0
Ga	50.0	50.0	50.0	50.0	70.0	80.0	50.0
Ge	< 10.0	20.0	< 10.0	< 10.0	100.0	20.0	< 10.0
Sn	< 10.0	50.0	100.0	200.0	150.0	70.0	100.0
W	< 20.0	20.0	30.0	< 20.0	30.0	< 20.0	< 20.0
Sb	32.5	68.7	27.0	23.3	7.72	8.03	17.3
Cs	58.6	2.17	14.05	12.92	1.51	11.91	11.06
Ba	3310.0	315.0	534.0	770.0	54.0	527.0	281.0
La	100.0	105.3	66.1	88.8	82.7	89.3	82.5
Ce	171.0	180.0	114.4	151.0	138.7	152.4	143.2
Nd	59.4	61.1	39.3	49.6	46.5	53.	49.5
Sm	10.32	10.46	6.87	8.80	7.87	9.06	8.41
Eu	1.80	1.89	2.30	3.26	4.79	3.40	3.80
Tb	0.771	0.765	0.439	0.548	0.510	0.746	0.593
Yb	1.10	0.91	0.46	0.48	0.66	0.84	0.71
Lu	0.135	0.112	0.063	0.064	0.093	0.096	0.101
Hf	5.01	5.76	3.57	4.28	4.02	4.60	4.46
Ta	3.58	3.87	2.76	2.95	2.70	3.09	3.03
Au	< 0.003	0.010	0.015	0.023	< 0.007	< 0.009	< 0.008
Th	23.8	27.1	16.7	20.0	19.2	21.9	20.0
U	9.87	11.10	8.41	8.66	7.47	9.1	8.42

Major element data by XRF, D.F. Siems and J.E. Taggart, analysts. Most trace element data by instrumental neutron activation analysis, J. Grossman, analyst; Ag, Be, Bi, Ga, Ge, Sn, and W by ICP optical spectroscopy, R.T. Hopkins, analyst

oxidized upper part of the orebody, and a zircon fission-track date of 12.0 ± 0.4 Ma. The Japan International Co-operation Agency (1985) reported a sericite age of 12.8 ± 0.6 Ma from the orebody, and Ueno and Sugaki (1984) reported an age on alunite of 7.5 ± 1.2 Ma. Grant et al. (1979) estimated a minimum age of 12.0 ± 0.2 Ma for the dacite and mineralization based on dating of a rhyolite ash-flow tuff (Huakachi Formation) that overlies the northern part of the Cerro Rico dome and which contains mineralized fragments of the dacite.

The samples collected for the present study are described in Table 1, their locations are plotted on Fig. 2, and major and selected trace element analyses are given in Table 3. Of these, sample M 6a was a special 100 kg sample of sericitized dacite that was collected from the high-temperature core to provide sufficient zircon for both U-Th-Pb and fission-track dating as well as sericite for K-Ar dating. Following the conventions of the individual laboratories, uncertainties are given as 2 standard deviations (2σ) for the U-Th-Pb ages, and as 1 standard deviation (1σ) for the K-Ar, Ar-Ar, and fission track ages.

U-Th-Pb dating

U-Th-Pb dating of zircon was used to establish the time of crystallization of the Cerro Rico dacite as well as to provide information about the source rocks of the magma.

Table 4. U-Th-Pb isotopic ages of zircon from Cerro Rico de Potosi, Bolivia

Sample number	Concentration (ppm)			Age (Ma)[a]			
	U	Th	Pb	$^{206}Pb/^{238}U$	$^{207}Pb/^{235}U$	$^{207}Pb/^{206}Pb$	$^{208}Pb/^{232}Th$
M 4	1112.3	510.7	3.626	18.2 ± 0.2	18.5 ± 0.3	64 ± 5	17.3 ± 0.2
M 5–1	1146.2	464.3	5.195	20.6 ± 0.3	21.4 ± 0.3	108 ± 12	18.4 ± 0.4
M 5–2[1]	1347.5	760.1	4.417	15.4 ± 0.1	15.5 ± 0.1	33 ± 7	15.3 ± 0.2
M 5–3[1]	1262.0	453.8	3.963	14.9 ± 0.2	15.0 ± 0.3	28 ± 9	14.5 ± 0.6
M 6[2]	1368.7	618.3	12.11	32.9 ± 0.2	55.3 ± 0.3	1178 ± 14	26.4 ± 0.5
M 6a–1[3]	1183.7	285.8	2.906	15.3 ± 0.2	15.5 ± 0.2	41 ± 7	15.3 ± 0.2
M 6a–2[3]	956.4	–	2.334	14.5 ± 0.1	14.6 ± 0.1	26 ± 5	–
M 6a–3[4]	922.1	401.8	2.081	13.8 ± 0.2	13.8 ± 0.3	22 ± 6	14.0 ± 0.3
M 6a–4[5]	792.2	608.3	3.136	23.0 ± 0.6	23.7 ± 0.6	91 ± 10	19.8 ± 0.5
M 6a–5[6]	2772.5	206.5	10.92	14.3 ± 0.4	14.4 ± 0.5	39 ± 18	5.9 ± 2.9[b]
M 6a–6[6]	1852.0	277.5	6.790	19.3 ± 0.2	19.7 ± 0.2	72 ± 9	22.2 ± 1.3
M 6a–7[2]	1217.0	230.8	3.693	18.1 ± 0.1	19.1 ± 0.1	150 ± 4	28.9 ± 0.2
M 6a–8[7]	1354.7	–	3.920	15.8 ± 0.2	16.0 ± 0.2	47 ± 8	–
M 6a–9[8]	765.6	156.7	2.525	21.1 ± 0.2	25.6 ± 0.3	480 ± 4	23.6 ± 0.3
M 6a–10[9]	549.1	56.0	1.933	14.4 ± 0.3	18.8 ± 0.4	620 ± 15	21.7 ± 1.2
M 6a–11[9]	276.9	39.4	1.981	14.5 ± 0.5	19.2 ± 0.6	657 ± 22	16.4 ± 2.0
M 7	1131.0	536.1	4.595	22.3 ± 0.2	23.8 ± 0.2	178 ± 6	18.7 ± 0.3
M 8	666.7	384.4	2.641	22.7 ± 0.5	25.0 ± 0.5	257 ± 9	21.6 ± 0.5

Decay constants: $^{238}U = 1.55125 \times 10^{-10}$ y^{-1}; $^{235}U = 9.8485 \times 10^{-10}$ y^{-1}; $^{232}Th = 4.9375 \times 10^{-11}$ y^{-1}; $^{238}U/^{235}U = 137.88$.
[a] Ages corrected for blank and common Pb; errors are 2 standard errors in millions of years. Isotopic composition of common lead is assumed to be $^{204}Pb:^{206}Pb:^{207}Pb:^{208}Pb = 1:18.78:15.68:39.07$ as determined on a coexisting pyrite from sample M-6a.
[b] Age strongly dependent on choice of common Pb. Samples are: [1]Yellow crystals; [2]Clear crystals; [3]Yellow, elongate crystals; [4]Tips of yellow, elongate crystals; [5]Yellow, equant crystals; [6]Abraded core of *single* yellow, equant crystal; [7]Clear, elongate crystals; [8]Clear, equant crystals; [9]Abraded core of *single* clear, equant crystal; Other samples were not differentiated on basis of color or elongation. For additional analytical data, see Zartman and Cunningham (1995)

Elaboration of this aspect of the investigation and a more detailed description of the analytical procedure appears in Zartman and Cunningham (1995). A summary of the U-Th-Pb isotopic data is given in Table 4 and plotted on a concordia diagram in Fig. 3.

The dacite contains a morphologically heterogeneous population of zircons with distinct variations in color from brownish-yellow to colorless, and a range in elongation from equant to greater than 10:1. Initial results obtained on bulk fractions of zircon from 4 samples of dacite (samples M 4, M 5, M 7, and M 8 (Table 4); stippled ellipses in Fig. 3) revealed the presence of a significant component of inherited, or relict, zircon, most likely as older cores that were overgrown by younger rims during the crystallization of the dacite magma. The dispersion of data on the concordia diagram indicates at least two ages of inherited zircon. Two additional analyses of yellow zircon (sample M 5, Table 4; solid ellipses in Fig. 3) further identify mixing between zircon that crystallized with the dacite and inherited zircon having an approximate age of 200 Ma. Colorless zircon from a fifth sample, M 6, contained a large proportion of the older inherited zircon, which could be extrapolated to an age of about 1.7 Ga.

In order to determine more precisely the crystallization, or emplacement, age of the dacite, it was deemed necessary to analyze selected fractions from a considerably larger sample. For this purpose, several milligrams of zircon were obtained from the 100-kg sample collected from the same locality as sample M 6 (hereafter referred to as sample M 6a). Based on variations in size, shape, and color, 9 fractions of sample M 6a zircons, weighing between 0.5 and 0.1 mg, were hand picked and analyzed (Table 4; Fig. 3). Previous studies have shown that the elongation of zircon crystals can be used to enhance or reduce the amount of the inherited component in a composite zircon crystal (Zartman et al. 1995). The more elongate the zircon, the less the amount of the inherited component, and crystals having a length-to-width ratio of greater than 6:1 indicate little or no such inheritance. Analysis of tips broken from the most elongate yellow crystals yielded the youngest U-Pb age of 13.8 ± 0.2 Ma, which we take as the best estimation of the crystallization age for the dacite.

To provide additional information about the age of the inherited components, two colorless and two yellow equant single crystals of zircon were abraded to remove rims, if present, and the remaining cores were analyzed (Table 4; Fig. 3). One of the yellow zircons revealed that it had crystallized entirely within the dacite magma, confirming the ~14 Ma age obtained previously. The other yellow zircon did have an inherited component, which, together with the other analyzed yellow fractions, gave a concordia upper intercept age of 191 ± 40 Ma. The cores of the colorless zircon also had inherited components suggestive of either an Archean age or postcrystallization disturbance of their isotopic systems (Zartman and Cunningham 1995).

K–Ar and $^{40}Ar/^{39}Ar$ dating

Eight samples of vein alunite, sericitized whole rock, and sericite separates were analyzed by conventional K-Ar techniques. Sample descriptions are in Table 1, sample

Table 5. K-Ar analytical data, Cerro Rico de Potosi, Bolivia

Sample number	Material dated	K_2O (%)	$^{*40}Ar$ moles/gram	$^{*40}Ar$ (%)	Age (Ma $\pm 1\sigma$)
M 1a	Alunite	10.78	9.7971×10^{-11}	71.9	6.3 ± 0.2
M 1b	Alunite	10.62	9.7241×10^{-11}	62.8	6.4 ± 0.2
M 2	Alunite	10.72	8.7499×10^{-11}	65.8	5.7 ± 0.2
M 3	Alunite	4.68	5.6210×10^{-11}	14.5	8.3 ± 0.5
M 4	Whole rock	2.71	2.85317×10^{-11}	4.6	7.3 ± 0.6
M 6	Sericite	8.93	1.72536×10^{-10}	52.9	13.4 ± 0.4
M 9	Sericite	7.37	1.11448×10^{-11}	33.3	10.5 ± 0.4
M 10	Sericite	8.23	1.3238×10^{-10}	71.3	11.1 ± 0.4

Values for constants used in calculating ages are as follows: $^{40}K\lambda_\epsilon = 0.581 \times 10^{-10}\ yr^{-1}$; $\lambda_\beta = 4.962 \times 10^{-10}\ yr^{-1}$; $^{40}K/K = 1.167 \times 10^{-4}$ The decay constants used for K and the abundance ratio $^{40}Ar/K_{tot}$ are those adopted by the International Union of Geological Sciences Subcommission on Geochronology (Steiger and Jäger 1977)

locations are plotted on Fig. 2, and the analytical data are in Table 5. Sericite from sample M 6a was selected for $^{40}Ar/^{39}Ar$ dating to define the timing of the main stage alteration and associated mineralization. The analytical data for this sample are given in Table 6, and the apparent ages are plotted as a function of thermal release of ^{39}Ar in Fig. 4. An $^{40}Ar/^{36}Ar$ versus $^{39}Ar/^{36}Ar$ isochron plot is shown in Fig. 5. These are the first $^{40}Ar/^{39}Ar$ determinations reported for Cerro Rico. The precision of the calculated age is the estimated analytical uncertainty in the measurement of the argon isotopes, radiogenic ^{40}Ar yield, and K_2O concentrations. Sample M 4 sericite is located above samples M1 and M 2 (Fig. 2) which give similar ages and may reflect local resetting. Samples M 9 and M 10 have slightly lower K_2 values which may reflect the presence of a minor contaminant such as quartz.

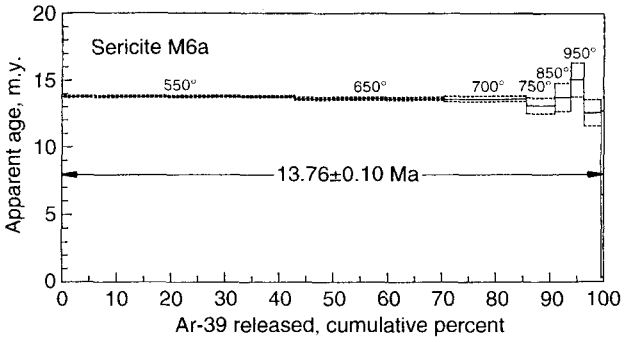

Fig. 4. High-precision, high-accuracy $^{40}Ar/^{39}Ar$ age spectra from sample M 6a sericite. Eight heating stages are shown as *horizontal bars*. Plateau release age is 13.76 ± 0.10 Ma

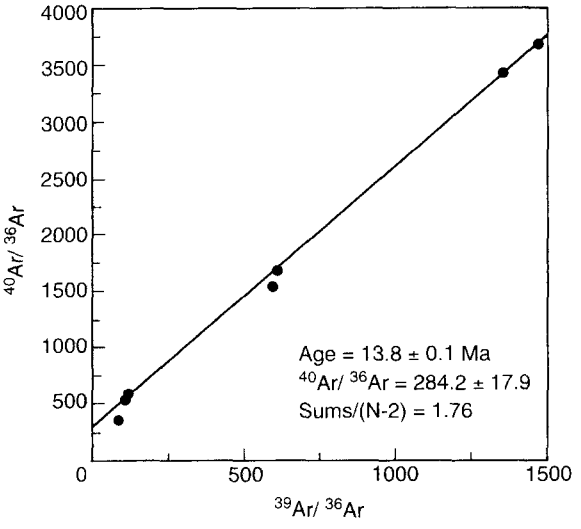

Fig. 5. $^{40}Ar/^{36}Ar$ versus $^{39}Ar/^{36}Ar$ isochron diagram for sample M 6a sericite. Isochron age is 13.8 ± 0.1 Ma

Fission-track dating

Fission-track studies of zircons from sample M 6a were made to investigate the thermal history of the Cerro Rico dome by the annealing of fission tracks. The zircons for this study were from the same sample M 6a that was used for the U-Th-Pb isotopic studies, and the K-Ar and $^{40}Ar/^{39}Ar$ dating. The fission-track data give a date of 12.5 ± 1.1 Ma (Table 7).

Table 6. $^{40}Ar/^{39}Ar$ analytical data from sample M 6a sericite, Cerro Rico de Potosi, Bolivia

Temp °C	$^{40}Ar/^{39}Ar$	$^{37}Ar/^{39}Ar$	$^{36}Ar/^{39}Ar$	$^{40}Ar^*$	^{39}Ar	Age (Ma $\pm 1\sigma$)
550	2.561	4.6×10^{-3}	7.4×10^{-4}	91.2	3.1×10^{-4}	13.8 ± 0.11
650	2.518	1.7×10^{-3}	6.8×10^{-4}	91.7	1.1×10^{-4}	13.6 ± 0.14
700	2.796	4.1×10^{-4}	1.6×10^{-3}	82.4	2.8×10^{-5}	13.7 ± 0.22
750	3.679	4.4×10^{-3}	4.9×10^{-3}	60.2	3.0×10^{-4}	13.1 ± 0.60
850	4.734	3.7×10^{-3}	8.1×10^{-3}	49.1	2.5×10^{-4}	13.8 ± 1.06
950	4.881	2.0×10^{-2}	7.9×10^{-3}	52.2	1.5×10^{-4}	15.1 ± 1.29
1100	2.627	8.1×10^{-3}	1.7×10^{-3}	80.9	5.4×10^{-4}	12.6 ± 1.00
1400	4.103	3.0×10^{-2}	1.1×10^{-2}	26.8	2.0×10^{-3}	6.5 ± 6.17

The J-value for all analyses is 0.003297. Reactor corrections: $(^{36}Ar/^{37}Ar)_{Ca} = 0.00027$, $(^{39}Ar/^{37}Ar)_{Ca} = 0.00067$, $(^{40}Ar/^{39}Ar)_K = 9.100 \times 10^{-3}$. The laboratory sample (93Y0090) was irradiated in the US Geological Survey TRIGA reactor (Denver, Colorado) for 16 h and the radiation flux was monitored using the Taylor Creek Rhyolite sanidine standard with an age of 27.92 Ma. The sample was heated by an induction coil with one-half hour heating steps and monitored by optical fiber thermocouple. Sample handling techniques and correction for Ca- and K-derived isotopes used in the Menlo Park laboratory are described by Dalrymple and Lanphere (1971, 1974). Isotopic analyses were made using a 60° sector, 15.2-cm-radius, Nier-type mass spectrometer

Table 7. Fission-track analytical data

Sample number	Material dated	ρs^a	ρi^b	Age (Ma $\pm 1\sigma$)
M 6a (DF-6443)	Zircon	3.86 (1073)	10.5 (610)	12.5 $\pm$ 1.1

[a] ρs, tracks/cm^2 fossil, $\times 10^6$; (number of tracks counted).
[b] ρi, tracks/cm^2 induced, $\times 10^6$; (number of tracks counted). 8 zircon grains; sample passed chi square test at 5% (external detector runs); muscovite dosimeter (SRM 962) density = 1.07×10^5 t/cm^2; 2697 tracks counted

Table 8. Summary of Cerro Rico de Potosi dates from this study

Method/Sample	Material dated	Age (Ma)
U-Pb		
M 6a	Zircon	13.8 $\pm$ 0.2 (2σ)
$^{40}Ar/^{39}Ar$		
M 6a	Sericite	13.76 $\pm$ 0.10 (1σ)
K-Ar		
M 1a	Alunite	6.3 $\pm$ 0.2 (1σ)
M 1b	Alunite	6.4 $\pm$ 0.2 (1σ)
M 2	Alunite	5.7 $\pm$ 0.2 (1σ)
M 3	Alunite	8.3 $\pm$ 0.5 (1σ)
M 4	Sericitized whole rock	7.3 $\pm$ 0.6 (1σ)
M 6a	Sericite	13.4 $\pm$ 0.4 (1σ)
M 9	Sericite	10.5 $\pm$ 0.4 (1σ)
M 10	Sericite	11.1 $\pm$ 0.4 (1σ)
Fission track		
M 6a	Zircon	12.5 $\pm$ 1.1 (1σ)

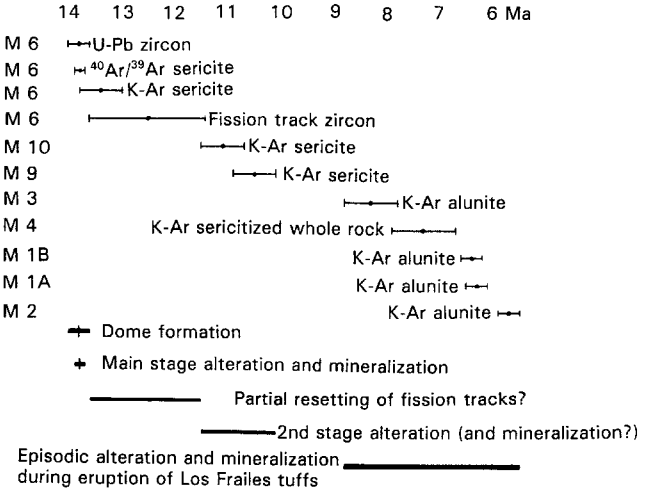

Fig. 6. Geochronology of Cerro Rico de Potosi, Bolivia

Discussion

The succession of volcanic strata in the vicinity of Cerro Rico de Potosi records a sequence of events that are interpreted to result from the eruption that culminated in a volcanic dome. The Pailaviri conglomerate is interpreted to be a basal lag conglomerate upon which the dome-related volcanic edifice was constructed. The Venus breccia (Fig. 2) consists of crudely horizontally bedded, fragments of the country rock as well as fragments of dacite that are interpreted to be from the solidified carapace of the dacitic magma, in a tuffaceous and comminuted country rock matrix. This breccia resulted from explosive activity and is interpreted as being caused by local phreatomagmatic explosions as the rising dacitic magma interacted with the ground water. This explosive activity released pressure and resulted in the rapid vesiculation of the volatile-rich top of the magma. This process recurred episodically yielding the well-bedded, locally cross-bedded, largely airfall, Caracoles tuff, forming a tuff ring over the Venus breccia. The plant-bearing lacustrine deposits present in the Caracoles tuff are interpreted to be local accumulations in an ephemeral lake that formed within the tuff ring. The largely devolatilized magma was then extruded out of the vent, flared outward over the tuff, and formed the Cerro Rico volcanic dome. Flow lines and quench textures are not apparent because of the annealing due to the heat in a dome this large, together with the effects of alteration and surface erosion. The sequence of events is similar to those related to dome explacement elsewhere in Bolivia (Cunningham et al. 1991a, b; Columba and Cunningham 1993; Pinto-Vásquez 1993). It is difficult to measure the amount of erosion that has taken place, but several lines of evidence suggest it has been not more than a few hundred meters. Nevertheless, erosion has been enough to modify the original dome morphology, changing it from a dome to a conical peak, but not sufficient to remove the silica cap that is interpreted to have formed at the top of the dome by hydrothermal processes shortly after the dome was extruded. Furthermore, the position of the ground surface at 12.0 $\pm$ 0.2 Ma is marked by the base of the Huakachi Formation ash-flow tuffs where they overlie the Cerro Rico Formation (Grant et al. 1979; Francis et al. 1981).

The geochronological data reported in this study, which are summarized in Table 8 and are shown graphically in Fig. 6, constrain the timing and thermal history of dome emplacement, alteration, and mineralization. The Cerro Rico dome was localized by a generally north-trending fault system, which was interpreted by Francis et al. (1981) to be a caldera ring fracture related to the Kari Kari caldera, whereas Bernstein and Harrington (1988) considered it to be a regional fault related to an anticlinal flexure. Although a caldera-related fracture could locally coincide with a regional fracture, recurrent movement of a regional nature is likely since the dome is 7 my younger than the caldera, and the dome was repeatedly fractured by recurrent fault movement over an additional 7 my.

Shortly after the dome was extruded at 13.8 $\pm$ 0.2 Ma, it was fractured by renewed movement on the fault system and a large, metal-bearing, hydrothermal system deposited ore and gangue minerals in the veins and caused pervasive alteration of the dacite. As a result, the dome was altered to a quartz-sericite-pyrite assemblage having a silicified cap. Although the paragenesis is complicated in detail by repeated cross-cutting events and variations in paragenetic relations attesting to recurrent episodes of mineralization and alteration, metal zoning at the scale of

the deposit suggests that there was only one major ore-forming event, and that this hydrothermal/mineralization event formed essentially all of the ore. The hydrothermal system was thermally and compositionally zoned, resulting in the deposition of a high-temperature mineral assemblage in the core and a lower-temperature mineral assemblage in the periphery. As the hydrothermal system cooled and collapsed, some of the lower temperature minerals characteristic of the peripheral zone were paragenetically superimposed, or telescoped, on higher temperature minerals of the core. The telescoped zoning pattern is similar to that observed at Julcani, southern Peru, where mineralization has been shown to be the result of mixing of high-level, evolved, magmatic fluids with meteoric water (Deen et al. 1994).

The minimum amount of time between dome extrusion and subsequent alteration/mineralization would be the amount of time it took for the dome to solidify. The sharp contacts of the veins and the through-going nature of the veins indicate the dome had sufficiently hardened to sustain fracturing.

The $^{40}Ar/^{39}Ar$ and fission-track dates place constraints on both the maximum amount of time it could have taken for the major part of the ore deposit to form and the maximum time/temperature parameters of any subsequent thermal events. Sample M 6a was collected from the high-temperature core of the deposit. The argon closure temperature of muscovite and sericite is affected chiefly by temperature but also to a small extent by cooling rate, being higher for fast cooling and lower for slow cooling (Dodson 1973). Detailed thermochronological studies of muscovite by Snee et al. (1988) have indicated muscovite closure temperatures of $\sim 325\,^{\circ}C$ during rapid cooling or as low as $\sim 270\,^{\circ}C$ during slow cooling or extended reheating. The sericite in sample M 6a is fine-grained, generally ~ 0.04 mm, and the pure sample analyzed was a 60–120 mesh (0.25–0.125 mm) fraction, so the analyzed grains were generally composite grains. This small grain size would increase the sensitivity to thermal diffusion because there would be less distance for Ar to diffuse and greater edge area. The major Ar release temperatures (Table 6 and Fig. 4) were low, with over 40% Ar released at 550 °C and about 85% released by 700 °C. This relatively low-temperature release from fine-grained sericite strongly indicates that there was no significant prolonged heating, or reheating associated with subsequent hydrothermal events after 13.76 ± 0.10 Ma, and that the main ore-forming event was a very short-lived event. It also confirms that the magmatic steam alunites, although perhaps as hot as 400 °C, were localized, brief bursts. The zircon fission track date of 12.5 ± 1.1 Ma indicates there was no significant heating ($> 240\,^{\circ}C$ for $> 10^4$ years; Hurford 1986; Naeser 1979) after this date, although the slightly younger zircon date may record the waning of the major hydrothermal system. The two samples of sericite (M9 and M10) that give ages of about 11 Ma are interpreted to represent a possible localized event that was not large enough to cause significant resetting. The maximum amount of time between volcanic dome extrusion and the formation of sericite during main-stage, high-temperature alteration/mineralization is calculated from the difference and analytical uncertainties between the ages of dome emplacement and sericitic alteration. Accordingly, for 13.8 ± 0.2 Ma $- 13.76 \pm 0.20$ Ma $= 0.04 \pm 0.28$ my (all uncertainties given here as 2σ values and $2\sigma_{12} = 2(\sigma_1^2 + \sigma_2^2)^{1/2}$), a maximum difference of ~ 0.3 my is derived at approximately the 95% confidence level.

The dome was repeatedly fractured as the fault system that initially guided the magma emplacement was episodically reactivated, both during the major mineralization event and during subsequent minor mineralization/alteration events. Such recurrent fault activity is indicated by cross-cutting vein relations and by K-Ar dates on younger sericite and alunite. The data suggest these events took place about 11 Ma, and then episodically from 8.3 to 5.7 Ma, the latter being the time of major volcanic activity in the adjacent Los Frailes volcanic field.

The stable isotope systematics of the alunites as well as those of the associated pyrite are typical of *magmatic steam* alunites that form in extensional environments usually at the end stages of hydrothermal systems (Rye et al. 1992; Rye 1993). The distinguishing stable isotope characteristics of these alunites are δD values indicating a magmatic source for the fluids and $\delta^{34}S$ values typical of the bulk sulfur in the system. Such alunites have been recognized as fracture fillings at Marysvale, Utah, Cactus, California, and Red Mountain, near Lake City, Colorado. They apparently formed intermittently during mineralization at El Indio, Chile (Raymond Jannes, oral communication 1994). Such alunites are believed to be related to bursts of evolved magmatic steam that escape during decompression of the magma. The magmatic steam travels so rapidly that the sulfur species (chiefly SO_2) in the magmatic vapor plume does not have time to reach isotopic equilibrium prior to precipitation of alunite (Rye 1993). The fluids flow so fast along extensional fractures that commonly even oxygen isotope equilibrium between SO_4 and OH in the precipitated alunite is not obtained. The fractionation of oxygen between SO_4 and OH is temperature dependent and the isotope data for samples M1 and M3 indicate temperatures of 290 and 240 °C. These are minimum temperatures, however, because of the possible oxygen isotope disequilibrium in the fluids during their ascent (Rye et al. 1992). Many magmatic steam alunites are believed to have formed near 400 °C, near the upper limit of alunite stability (Hemley et al. 1969). The process by which SO_2 is oxidized to SO_4^{-2} is not understood but is believed to be related to the loss of H_2 in the vapor phase and cooling.

The aforementioned constraints from the $^{40}Ar/^{39}Ar$ dated sericite corroborates the interpretation that the moderately high-temperature alunite veins were formed essentially instantaneously. The formation of these alunites about 7 my after main stage mineralization at Cerro Rico de Potosi requires a younger magma at depth whose evolved fluids were released episodically by sudden decompression. The relation of these young alunites at Cerro Rico de Potosi to possible mineralization at depth has not been fully explored.

Geochronology provides information that is useful for exploration and resource assessment. Precious metal mineralization in volcanic domes is generally associated with either acid sulfate or adularia-sericite alteration (Heald et al. 1987). In many cases, mineralization follows soon

after dome extrusion, reflecting a relation to the same magmatic/hydrothermal system at depth. Examples include Kori Kollo-La Joya, Bolivia, where the age of volcanism, sericite alteration, and mineralization is indistinguishable (Redwood 1987; Columba and Cunningham 1993), and Julcani, Peru, where volcanic domes, acid-sulfate alteration, and related mineralization occurred within a span of 0.5 my (Noble and Silberman 1984; Deen et al. 1994). Large adularia-sericite hydrothermal systems in volcanic domes form silicified caps because silica released by the alteration process (Meyer and Hemley 1967) generally moves upward and outward into cooler zones where it is deposited. Such caps are useful exploration guides.

Dating mineralizing episodes at Cerro Rico has exploration significance for the Los Frailes volcanic field, which covers a large area within the tin belt, just to the west of Cerro Rico (Fig. 1). The volcanic field consists chiefly of a sequence of peraluminous ash-flow tuffs, up to 800 m thick, that was erupted between 8 and 5 Ma from several sources (Evernden et al. 1977; Schneider 1985; Ericksen et al. 1990). Most of the ore at Cerro Rico, as well as that of other major metalliferous deposits in the central part of the Bolivian tin belt, is older than the Los Frailes ash-flow tuffs, suggesting similar deposits might exist beneath the ash-flow tuffs of the volcanic field. The Los Frailes tuffs contain anomalous concentrations of tin as well as widespread wood-tin and uranium occurrences. Ericksen et al. (1990) have suggested that the eruptive centers that were the sources of the tuffs may have intrusions with associated tin veins.

Both the dacitic magma and the metal-bearing hydrothermal solutions at Cerro Rico were clearly related to a larger magmatic/hydrothermal system at depth. The sources of the magma and metals, and the processes that they have been affected by, may be deduced both from rare earth element (REE) data as well as the Precambrian ancestry of zircon shown by U-Th-Pb isotopic systematics of this study. Five of the seven rock samples show chondrite-normalized REE patterns with LREE enrichment (high La_N/Yb_N ratio) and a significant Eu enrichment (Table 3, Fig. 7) in marked contrast to other igneous rocks in the tin belt that have negative Eu anomalies (G. Ericksen and R. Luedke unpublished data). The exceptions, samples M4 and M5, are at the highest elevations in the dome and may reflect either inhomogeneity in the magmatic/hydrothermal system, effects of oxidation, or the overprint of younger hydrothermal systems (M 4 has been dated at 7.3 Ma and is located approximately above the similar-age magmatic-steam vein alunites). Because the dacite is extensively altered, the Eu enrichment could have been inherited from the REE concentration in the dacitic magma, the REE concentration in the hydrothermal fluids, or both; although, based on a comparison with REE patterns of fresh rocks from other deposits in the tin belt, it is probably due to the hydrothermal fluids. Eu can be concentrated several ways. One way is that plagioclase feldspars that concentrated Eu from their parent magma during crystallization (Graf 1977) and settled in the base of a nearby magma chamber, which then solidified, could serve as a source of Eu-enriched fluids. A possible candidate is the pluton that underlies the adjacent Kari Kari caldera. An alternative source of LREE enriched fluids with a high Eu content is deep-crust, tonalite-trondhjemite rocks of Precambrian age (Weaver and Tarney 1981; Tarney and Jones 1994) that could be involved in the subduction zone; these rocks, with their REE concentrations, may ultimately have been derived from mafic sources (Bau 1991; Rollinson 1994).

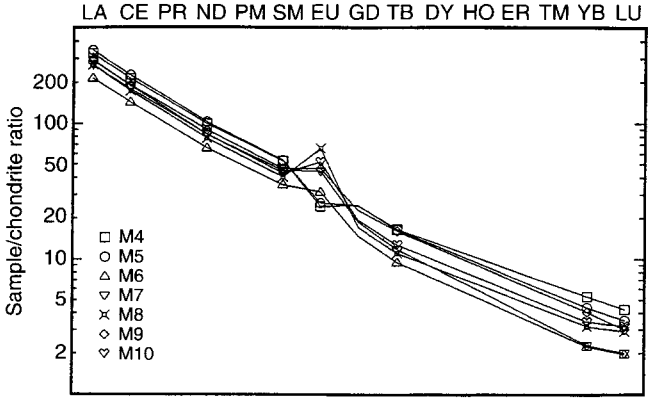

Fig. 7. Chondrite-normalized rare earth element (REE) plot of analyzed samples

Tin is effectively transported in hydrothermal solutions under conditions similar to those that enhance Eu^{+2} solubility. It appears that tin may have been transported in a hydrothermal solution, together with Eu^{+2}, with the peraluminous magmas under the reduced conditions of the black phyllites (Lehmann 1990, 1994). Deposition would be due to a decrease in temperature, increase in Ph, or increase in oxygen fugacity such as by a redox reaction by coupled precipitation with sulfides or mixing with meteoric waters (Wilson and Eugster 1990).

The abundance of tin at Cerro Rico and elsewhere in the tin belt provides additional insight into the sources of the peraluminous igneous rocks with which the tin deposits are associated. Tin is present in deposits ranging in age from Middle Triassic to late Tertiary, suggesting that tin was episodically remobilized in this metallogenic province. Metasedimentary rocks might have been a source of high-alumina, low-oxygen fugacity, ilmenite-series magma that underwent fractional crystallization and formed the igneous rocks of the tin belt (Ishihara 1977; Halls and Schneider 1988; Avila-Salinas 1990; Lehmann 1990, 1994; and Aitcheson et al. 1995). In the Precambrian craton to the east, large tin deposits, such as those in the Rondônia and Mapuera districts of Brazil, (Ljunggren 1964; Thorman and Drew 1988), have ages similar to the Precambrian ages for some of the inherited zircons described in this report. Tin-bearing granoblastic to gneissic lithic inclusions, which have been found in the Morococala volcanic field within the tin belt about 200 km north of Cerro Rico (Ericksen et al. 1990), might have come from such rocks. Another possible tin source might have been Precambrian remobilized tin placers (alluvial concentrates) along the edge of the craton (Ljunggren 1964; Schneider and Lehmann 1977). Such Precambrian rocks might have been sources for both tin and enriched Eu as well as the inherited Precambrian zircon.

Conclusions

Cerro Rico de Potosi, the world's largest silver deposit, formed in what is interpreted to be a dacite volcanic dome, shortly after the dome was extruded. It is a zoned ore deposit having a high temperature Sn-W-Bi core surrounded by a lower temperature Ag-Pb-Zn mineral assemblage that was superimposed, or telescoped, on the core as the hydrothermal system waned. U-Th-Pb dating of the tips of elongate zircon crystals show the dome was extruded at 13.8 ± 0.2 Ma. This is believed to be the youngest volcanic rock to be studied in such detail by the U-Pb zircon technique. Pervasive quartz-sericite-pyrite alteration accompanied mineralization and formed a silica cap on the dome, part of which still remains. $^{40}Ar/^{39}Ar$ dating of sericite from deep within the core indicates main stage alteration at Cerro Rico occurred at 13.76 ± 0.1 Ma, essentially immediately after the dome was extruded and hardened. The exceptionally flat Ar release pattern shows there was no significant heating afterwards. Fission track dating of zircons from the same sample gives a date of 12.5 ± 1.1 Ma that corroborates the $^{40}Ar/^{39}Ar$ data and provides additional insight into the waning of the hydrothermal system. Subsequent hydrothermal events, including bursts of magmatic steam, about 11 Ma and between 8.3 and 5.7 Ma were not hot enough for enough time to be significant thermal events.

U-Th-Pb isotopes and a positive Eu anomaly provide information about possible sources of magma, hydrothermal fluids, and metals, as well as the processes involved in concentrating them. Both the Cerro Rico volcanic dome and the ore deposit were formed from a larger magmatic-hydrothermal system at depth and the geochronological data document the close temporal association of the magmatic and hydrothermal systems. U-Th-Pb dating of zircon crystals indicates the presence of a component dated at 1.7 Ga, indicating a Precambrian heritage and thus the probable influence of the western edge of the Precambrian craton in magma generation.

Acknowledgements. Many people helped to make this study possible. We especially appreciate the assistance of Alfonso Leaño R. and Jhonny Gamón of Corporacion Minera de Bolivia, Empresa Minera Subsidiaria Potosi, and Jim McNamee of Compañia Minera del Sur S.A., for their help with access to mine maps and obtaining samples; Gerry Cebula for an outstanding job of mineral separations; Bob Seal for his excellence with microprobe analyses of minerals in alunite veins; George Steele, who is doing his Ph. D. Thesis at the University of Aberdeen on Cerro Rico, for his insight into mineral paragenesis and thoughtful review of the manuscript; and to Robert Ayuso, Paul Barton, Merwin Bernstein, Chris Halls, Doug Haynes, Chris Henry, Robert Luedke, Michael Kunk, Stewart Redwood, Clive Rice, and Dieter Wolf for stimulating discussions and reviews of the manuscript.

References

Ahlfeld, F. (1967) Metallogenetic epochs and provinces of Bolivia. Mineral. Deposita 2:291–311

Ahlfeld, F., Schneider-Scherbina, A. (1964) Los yacimientos minerales y hidrocarburos de Bolivia. Bolivia Departmento Nacional de Geologia, Boletin 5, 388 pp

Aitcheson, S.J., Harmon, R.S., Moorbath, S., Soler, P., Soria-Escalante, E., Steele, G., Swainbank, I., Wörner, G. (1995) Pb isotopes define basement domains of the Altiplano, central Andes. Geology 23:555–558

Avila-Salinas, W.A. (1990) Tin-bearing granites from the Cordillera Real, Bolivia; a petrological and geochemical review. In: Kay, S.M., Rapela, C.W., (eds.) Plutonism from Antarctica to Alaska. Geol. Soc. Am. Spec. Paper 241:145–159

Bau, M. (1991) Rare-earth element mobility during hydrothermal and metamorphic fluid-rock interaction and the significance of the oxidation state of europium. Chem. Geol. 93:219–230

Bernstein, M. (1987) Considerations for the future Bolivian Industry; profitable mines through economy of scale. 1986 Internal Report prepared for the Mining Industry Task Force, Ministerio de Minas, La Paz, Bolivia

Bernstein, M. (1989) Expectations for bulk tonnage hard rock and alluvial ores. United Nations Development Program, Project BOL/87/012, La Paz, Bolivia, 18 pp

Bernstein, M., Harrington, R. (1988) Observations on the economic geology and volcanic setting of Cerro Rico de Potosi. IUGS/UNESCO Deposit Modeling Workshop, Hydrothermal systems in Volcanic centers, September 4–16, 1988, La Paz, Bolivia

Berry, E.W. (1939) The fossil flora of Potosi, Bolivia. The Johns Hopkins Univ. Studies in Geol. 13:9–67

Brüggen, J. (1934) Grundzüge der Geologie und Lagerstättenkunde Chiles. Heidelberg, 91 pp

Columba C.M., Cunningham, C.G. (1993) Geologic model for the mineral deposits of the La Joya district, Oruro, Bolivia. Econ. Geol. 88:701–708

Cunningham, C.G., Ericksen, G.E. (1991a) Exploration guides for precious-metal deposits in volcanic domes. In: Good, E.E., Slack, J.F., Kotra, R.K. (eds.) Seventh Ann. V.E. McKelvey Forum on Mineral and Energy Resources. U.S. Geol. Surv. Circ. 1062:23–24

Cunningham, C.G., McNamee, J., Pinto Vásquez, José, Ericksen, G.E. (1991b) A model of volcanic dome-hosted precious metal deposits in Bolivia. Econ. Geol. 86:415–421

Dalrymple, G.B., Lanphere, M.A. (1971) $^{40}Ar/^{39}Ar$ technique of K-Ar dating – A comparison with the conventional technique. Earth Planet. Sci. Lett. 12:300–308

Dalrymple, G.B., Lanphere, M.A. (1974) $^{40}Ar/^{39}Ar$ age spectra of some undisturbed terrestrial samples. Geochim. Cosmochim. Acta 38:715–738

Deen, J.A., Rye, R.O., Munoz, J.L., Drexler, J.W. (1994) The magmatic-hydrothermal system at Julcani, Peru: Evidence from fluid inclusions and hydrogen and oxygen isotopes. Econ. Geol. 89:1924–1938

Dodson, M.H. (1973) Closure temperature in cooling geochronological and petrological systems. Contrib. Mineral. Petrol. 40:259–274

Ericksen, G.E., Luedke, R.G., Smith, R.L., Koeppen, R.P., Urquidi B.F. (1990) Peraluminous igneous rocks of the Bolivian tin belt. Episodes 13:3–7

Evans, D.L. (1990) Structure and mineral zoning of the Pailaviri section, Potosi, Bolivia. Econ. Geol. 35:737–750

Evernden, J.F., Kriz, S.J., Cherroni, M.C. (1977) Potassium-argon ages of some Bolivian rocks. Econ. Geol. 72:1042–1061

Francis, P.W., Baker, M.C.W., Halls, C. (1981) The Kari Kari caldera, Bolivia, and the Cerro Rico stock. J. Vol. Geotherm. Res. 10:113–124

Graf, J.L. Jr. (1977) Rare earth elements as hydrothermal tracers during the formation of massive sulfide deposits in volcanic rocks. Econ. Geol. 72:527–548

Grant, J.N., Halls, C., Avila Salinas, W., Snelling, N.J. (1979) K-Ar ages of igneous rocks and mineralization in part of the Bolivian tin belt. Econ. Geol. 74:838–851

Halls, C., Schneider, A. (1988) Comentarios sobre la génesis de los yacimientos del cinturón estañifero boliviano. Rev. Geol. Chile 15:41–56

Heald, P., Foley, N.K., Hayba, D.O. (1987) Comparative anatomy of volcanic-hosted epithermal deposits: Acid-sulfate and adularia-sericite types. Econ. Geol. 82:1–26

Hemley, J.J., Hostetler, P.B., Gude, A.J., Mountjoy, W.T. (1969) Some stability relations of alunite. Econ. Geol. 64:599–612

Hurford, A.J. (1986) Cooling and uplift patterns in the Lepontine Alps, South Central Switzerland and an age of vertical movement on the Insubric fault line. Contrib. Mineral. Petrol. 92:413–427

Ishihara, S. (1977) The magnetite-series and ilmenite-series granitic rocks. Mining Geol. 27:293–305

Japan International Cooperation Agency (1985) K-Ar ages of mineralization at the Caracoles, Siglo XX, Colquechaca, Huari Huari, Unificada, Tasna, Inocentes and Buena Vista mines in Bolivia. In. Proy. Inst. Geol. Econ. Universidad Mayor de San Andres de Bolivia, 2, 270–280

Lehmann, B. (1990) Metallogeny of tin. In: Bhattacharji, S., Friedman, G.M., Neugebauer, H.J., Seilacher, A. (eds.) Lecture notes in Earth Sciences, 32. Springer, Berlin Heidelberg New York, 211 p

Lehmann, B. (1994) Petrochemical factors governing the metallogeny of the Bolivian tin belt. In: Reutter, K.J., Scheuber, E., Wigger, P.J. (eds.) Tectonics of the Central Andes. Springer, Berlin Heidelberg New York, pp. 317–326.

Lindgren, W., Creveling, J.G. (1928) The ores of Potosi, Bolivia. Econ. Geol. 55:233–262

Ljunggren, P. (1964) The tin deposits of Rondônia, Brazil, as compared with the Bolivian mineralization. Geol. Fören. Stockholm Förh. 85:431–435

Meyer, C., Hemley, J.J. (1967) Wall rock alteration. In: Barnes, H.L. (ed.) Geochemistry of hydrothermal ore deposits, Holt, Rinehart and Winston, New York, pp. 166–235

Miller, B., Singewald, J. (1919) The mineral deposits of South America. McGraw-Hill 597 pp

Naeser, C.W. (1979) Fission-track dating and geologic annealing of fission tracks. In: Jäger, E., Hunziker, J.C. (eds.) Lectures in isotope geology. Springer, Berlin Heidelberg New York, pp. 154–169

Noble, D.C., Silberman, M.L. (1984) Evolutión volcánica é hidrotermal y cronologia de K-Ar del distrito minero de Julcani, Peru. Bol. Soc. Geol. Perú, vol jubilar, LX Aniversario 5:1–35

Omiste, M. (1893) Cronicas Potosinas. Editora "El Siglo Ltda.", Potosi, Bolivia

Pinto-Vásquez, J. (1993) Volcanic dome-associated precious and base metal epithermal mineralization at Pulacayo, Bolivia. Econ. Geol. 88:697–700

Redwood, S.D. (1987) The Soledad caldera, Bolivia: A Miocene caldera with associated epithermal Au-Ag-Cu-Pb-Zn mineralization. Geol. Soc. Am. Bull. 99:395–404

Rollinson, H. (1994) Origin of felsic sheets in the Scourian granulites: new evidence from rare earth elements. Scot. J. Geol. 30:121–129

Rye, R.O. (1993) The evolution of magmatic fluids in the epithermal environment: the stable isotope perspective. Econ. Geol. 88: 733–753

Rye, R.O., Bethke, P.M., Wasserman, M.D. (1992) The stable isotope geochemistry of acid sulfate alteration. Econ. Geol. 87:225–262

Schneider, A. (1985) Eruptive processes, mineralization and isotopic evolution of the Los Frailes Karikari region/Bolivia. Unpublished Ph. D. Dissertation, Imperial College, University of London, England

Schneider, A. (1987) Eruptive processes, mineralization and isotopic evolution of the Los Frailes Karikari region, Bolivia. Rev. Geol. Chile 30:27–33

Schneider, A., Halls, C. (1985) Chronology of eruptive processes and mineralization of the Frailes Karikari volcanic field; eastern cordillera, Bolivia. Comunicaciones 35:217–224

Schneider, H.J., Lehmann, B. (1977) Contribution to a new genetical concept on the Bolivian tin province. In: Klemm, D.D., Schneider, H.J. (eds.) Time- and stratabound ore deposits. Springer, Berlin Heidelberg New York, pp. 153–168.

Sillitoe, R.H., Halls, C., Grant, J.N. (1975) Porphyry tin deposits in Bolivia. Econ. Geol. 70:913–927

Snee, L.W., Sutter, J.F., Kelly, W.C. (1988) Thermochronology of economic mineral deposits: dating the stages of mineralization at Panasqueira, Portugal, by high-precision $^{40}Ar/^{39}Ar$ age spectrum techniques on muscovite. Econ. Geol. 83:335–354

Steiger, R.H., Jäger, E. (1977) Subcommission on geochronology; convention on the use of decay constants in geo- and cosmochronology. Earth Planet. Sci. Lett. 36:359–362

Steinmann, Gustav (1922) Über die junge Hebung der Kordillere Südamerikas. Geol. Runds. 13:1–8

Stoffregen, R.E. (1987) Genesis of acid sulfate alteration and Au-Cu-Ag mineralization at Summitville, Colorado. Econ. Geol. 82: 1575–1591

Stoffregen, R.E., Rye, R.O., Wasserman, M.D. (1994) Experimental studies of alunite I. ^{18}O and D fractionation factors between alunite and water at 250–450 °C. Geochem. Cosmochim. Acta 58:903–916

Sugaki, A., Kojima, S., Shimada, N. (1988) Fluid inclusion studies of the polymetallic hydrothermal ore deposits in Bolivia. Mineral. Deposita 23:9–15

Sugaki, A., Ueno, H., Shimada, N., Kusachi, I., Kitakaze, A., Hayashi, K., Kojima, S., Sanjines V.O. (1983) Geological study on the polymetallic ore deposits in the Potosi district, Bolivia. Science Reports Tohoku University, Series III 15:409–460

Suttill, K.R. (1988) Cerro Rico de Potosi. Eng. Min. J. March 1988, pp. 50–53.

Tarney, J., Jones, C.E. (1994) Trace element geochemistry of orogenic igneous rocks and crustal growth models. J. Geol. Soc. London 151:855–868

Thorman, C.H., Drew, L.J. (1988) A report on site visits to some of the largest tin deposits in Brazil. U.S. Geol. Surv. Open-File Rep. 88–0594, 19 p

Turneaure, F.S. (1960a) A comparative study of major ore deposits of central Bolivia. Part I. Econ. Geol. 55:217–254

Turneaure, F.S. (1960b) A comparative study of major ore deposits of central Bolivia. Part II. Econ. Geol. 55:574–606

Turneaure, F.S. (1971) The Bolivian tin province. Econ. Geol. 66: 215–225

Turneaure, F.S., Marvin, T.C. (1947) Notas perliminares sobre la geologia del distrito de Potosi. Mineria Boliviana 36:3–8

Ueno, H., Sugaki, A. (1984) K-Ar ages of mineralization at the Morocala, Avicaya, Bolivar, Unificada, Chorolque and Tasna mines in Bolivia: Ann. Rep. JICA (Japan International Cooperation Agency) and UMSA (Universidad Mayor de San Andres), Part II 1:1162–1170

Urquidi-Barrau, F. (1989) Tin and tungsten deposits of the Bolivian tin belt. In: Ericksen, G.E., Cañas Pinochet, M.T., Reinemund, J.A. (eds.) Geology of the Andes and its relation to hydrocarbon and mineral resources. Houston, Texas. Circum-Pacific Council for Energy and Mineral Resources Earth Science Series 11: 313–323

Weaver, B.L., Tarney, J. (1981) Lewisian gneiss geochemistry and Archean crustal development models. Earth Planet. Sci. Lett. 55: 171–180

Wilson, G.A., Eugster, H.P. (1990) Cassiterite solubility and tin speciation in supercritical chloride solutions. In: Spencer, R.J., Chou, I-Ming (eds.) Fluid-mineral interactions: a tribute to H.P. Eugster. Geochem. Soc. Spec. Pub. 2:179–195

Zartman R.E., Cunningham, C.G. (1995) U-Pb zircon dating of the 13.8-Ma dacite volcanic dome at Cerro Rico de Potosi, Bolivia. Earth Planet. Sci. Lett. 133:227–237

Zartman, R.E., Dyman, T.S., Tysdal, R.G., Pearson, R.C. (1995) U-Pb ages of volcanogenic zircon from porcellanite beds in the Vaughn Member of the mid-Cretaceous Blackleaf Formation, southwestern Mont.: US Geol. Surv. Bull. 2113-B, p. B1–B16

Editorial handling: B. Lehmann